Microcavity Fiber Fabry–Pérot Interferometer With an Embedded Golden Thin Film

Cheng-Ling Lee, Jui-Ming Hsu, Jing-Shyang Horng, Wei-Yi Sung, and Chai-Ming Li

***Abstract*— We propose an ultracompact microcavity fiber Fabry–Pérot interferometer (MCFFPI) based on an ultrathin film of gold (Au) embedded in a single-mode fiber endface. The embedded Au thin film splits the input light into two paths for interference. The interference fringes of the proposed configuration with different cavity lengths are observed experimentally, and we verify that the interference patterns are from a combination of the Au-embedded reflector and Fresnel reflection of fiber endface. The MCFFPIs are further applied to measure the external refractive index (RI) of surrounding and for high temperature (T) sensing. Experimental results show that an excellent sensitivity of the RI sensing and a good linearity response of high temperature measurement are achieved.**

***Index Terms*— Fiber-optic component, fiber–optic sensor, microcavity fiber Fabry–Pérot interferometer (MCFFPI), thin film.**

I. Introduction

PROBE TYPES of miniature Fiber Fabry–Pérot interferometers (MFFPIs) are extremely important in many sensing applications especially for exploring some physical parameters in the dangerous environments and in the micro-specimens. Numerous MFFPIs with smart, simple and hybrid structures for these fields of applications on various parametric sensing have been proposed [1]–[13]. The MFFPIs devices can be used to measure external refractive index (RI) [1]–[4], ambient temperature (T) [5]–[8], pressure [9]–[10], strain [11] and other parameters like humidity [12] or high frequency ultrasonic wave [13]. The sensing characteristics of these tip typed MFFPI sensors are generally sensitive, probing configuration and ultracompact by use of techniques: fusion splicing different kinds of fibers [2], [6], chemical etching [10], femto-second laser machining [3]–[4], special splicing techniques to form air-gap or air-bubble [11] and combining with other materials [1], [5], [7]–[9], [12]–[13]. The structure of these MFFPIs can achieve the well known two modes interference mechanism and obtain low finesse interferometric characteristics. In addition, the sensor head of the MFFPIs with fiber tip structures are much more convenient and ultracompact, such properties will be very useful as a sensing probe for detecting in the pernicious conditions. Although many probe types of MFFPIs cooperated with other materials for enhancing sensitivities have been reported recently. However, some used materials are not suitable for high T sensing which may reduce the functional flexibilities of the measurements in practical applications [1], [5], [7]–[8].

In the present Letter, a new configuration of miniature, microcavity FFPI (MCFFPI) based on an ultrathin gold (Au) film embedded in the endface of fiber is investigated. Although, two TiO_2 dielectric thin films embedded in the fiber with a certain length to make an F-P cavity for measuring temperature and laser wavelength was firstly reported by Prof. Henry F. Taylor *et al.* [14]. Later, a similar work of the TiO_2 dielectric thin film to form as a miniature fiber optic interferometer for high temperature sensing up to 500 °C has been also investigated [15]. However, our miniature MCFFPI sensor with the probe typed configuration used as a simple refractometer also to be a high T sensor is much attractive in the practical applications. Based on the experimental results, the sensing characteristics of our device can be applied to measure external RI of surrounding with high sensitivity and also for high T sensing with good linearity, repeatability and stability responses.

II. MCFFPI Configuration and Principle of Operation

In the experiment, the metal Au was firstly coated on a fiber endface by high-vacuum RF-magnetron sputtering. The original Au film with thickness of about 50nm on a single mode fiber (SMF-28) endface is shown in Fig. 1(a). The Au-coated SMF fusion splices a non-coated SMF Fig. 1(b) to obtain reflection of about 0.01 so that can estimate the thickness of Au thin film is reduced lower than 5nm (almost disappear). The fusion splicing was accomplished by a commercial splicer, Ericsson FSU975. By editing the SM+SM(01) original program in the splicer, the arc current and duration are modulated and operated at lower level so that the Au thin film is retained a little after splicing to produce a small reflection. Even so, the proposed device will be suffered high splicing loss if the coated and non-coated SMFs having a misaligned fusion splicing. The embedded ultrathin film of Au in the SMF with successful splicing is obtained as displayed in Fig. 1(c). Afterward we can fabricate arbitrary length of F-B cavity in the proposed Au embedded MCFFPI by cleaving any one side of the SMF. In Fig. 1(d), the red and green lines respectively show the reflections of the original and after fusion splicing of the Au thin film. The dashed line

Manuscript received February 7, 2013; accepted March 6, 2013. Date of publication March 19, 2013; date of current version April 10, 2013. This work was supported by the National Science Council of China under Grant NSC100-2221-E-239-038 and Grant NSC101-2221-E-239-020.

The authors are with the Department of Electro-Optical Engineering, National United University, Miaoli 360, Taiwan (e-mail: cherry@nuu.edu.tw; jmhsu@nuu.edu.tw; jshorng@nuu.edu.tw; sqwexasd@yahoo.com.tw; cool018104@hotmail.com).

Color versions of one or more of the figures in this letter are available online at http://ieeexplore.ieee.org.

Digital Object Identifier 10.1109/LPT.2013.2252612

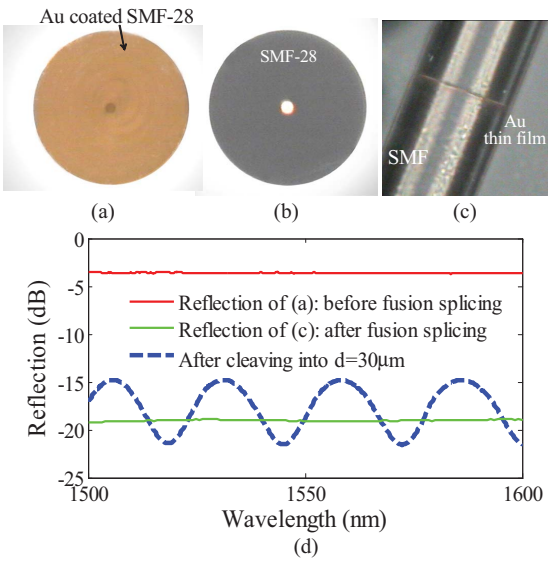

Fig. 1. Micrographs of cross-sectional SMF with (a) Au-coated, (b) non-coated, and (c) after fusion splicing. (d) Measurement of spectral reflections of (a), (c) and an MCFFPI device with $d = 30\ \mu$m.

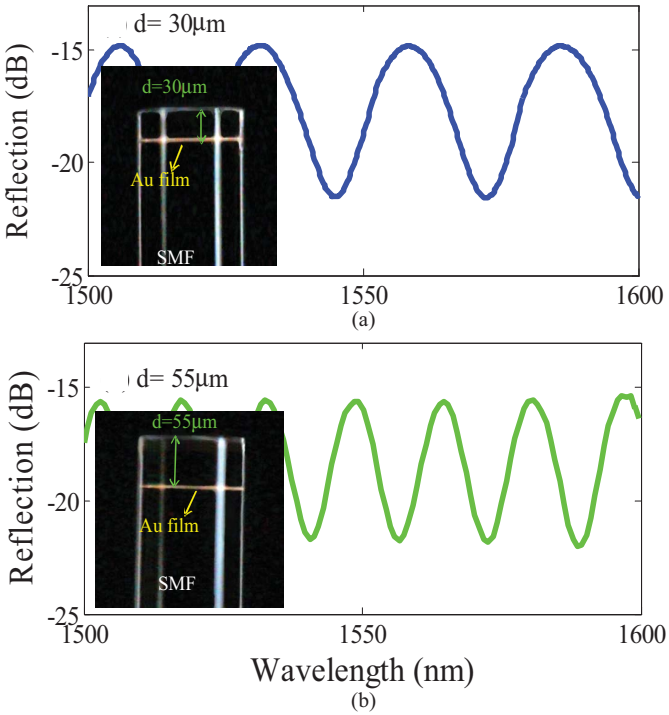

Fig. 2. Experimental reflection spectra of the devices in air and at $T = 25$ °C with cavity length d. (a) 30 μm. (b) 55 μm. Insets: corresponding fiber tip structures of the Au-embedded MCFFPIs.

shows the reflection of the fabricated MCFFPI by cleaving into a desired cavity length (d) of about 30 μm. The result performs a sinusoidal spectral response due to the low finesse Fabry–Pérot interference (it also can be modeled by two-beam interference mechanism). Here the embedded Au thin film splits the optical power into two segments, named reflection power of ultrathin film of the Au (r_1) and sensor endface (r_2), which travels through the F-B cavity for recombining and interfering. Here, the SMF endface acts like the Fresnel mirror based on the Fresnel reflection and the r_2 can be roughly estimated as ~$|(n(\lambda)\text{-}n_D(\lambda))/(n(\lambda)+n_D(\lambda))|^2$. Here the value of n_D denotes the RI of the used liquids (surrounding) which is measured at 25 °C, Sodium D Line, 589.3 nm. n is effective index of the core mode which is ~1.46 at wavelength (λ) around 1550nm makes r_2~0.036 in the air to combine r_1 in the launched SMF and interfere. Fig. 2 shows the reflection spectra of various cavities of the fabricated MCFFPIs in the air and at T = 25 °C. The spectra are measured by an optical spectrum analyzer (OSA) from launching a broadband light source (BBS). The used BBS contains a set of SLEDs (super-luminescent light emitting diodes) which is from the Opto-Link Corporation Ltd. In the insets, the shine of the Au thin film is observed even that is ultrathin. One can see that the fiber tip with very miniature structure can be effectively controlled and fabricated by a commercial cleaver, Fujikura CT-07. This fiber cleaver with a transparent window on the side can make users to see the splicing junction of the sensor clearly. Based on our experiences, by skillfully controlling the position of the junction (very near the Au thin film) with corrected cleaving, we can successfully fabricate the flat fiber tip with such a tiny cavity within the maximum error of about $\pm 10\mu$m with high repeatability.

In the Fig. 2 (a) and (b), the spectral fringes show a good sinusoidal interference curve and a fair extinction ratio (ER) with about 6~7dB (i.e. fringe contrast) since the r_1 and r_2 are small as well as with different intensities to make the interference pattern weak. The reflection spectra of the interference from the two different reflections (r_1 and r_2) in the F-B cavity can be expressed below [4]

$$R = \frac{r_1 + r_2 + 2\sqrt{r_1 r_2}\cos(\delta)}{1 + r_1 r_2 + 2\sqrt{r_1 r_2}\cos(\delta)} \tag{1}$$

where r_1 is reflection of the first interface (Au ultrathin film), r_2 is reflection of the fiber endface. The $\delta = (2\pi/\lambda)\cdot 2nd$ denotes the phase difference of the cavity, and d represents length of the microcavity. The numerical results of the MCFFPI with d = 55μm are ideally achieved by use of the Eq. (1) and calculated results are shown in the Fig. 3(a). One can see in the figure, the ER of the interference fringes is getting small when the external RI is increasing.

III. Experimental Results and Discussion

To investigate the RI sensing characteristics of the proposed MCFFPI as a probe-typed refractometer, an Cargille optical index liquid that is used for achieving the standard and precise RI measurement. During the measurement, the T(°C) is fixed and controlled by a TE cooler (resolution: 0.02 °C). As we can see in Fig. 3(b), when the fiber probe is immersed in an extremely small drop of the liquid of $n_D = 1.3$, the contrast of the interference fringes only has a little change but with high loss of fringe peak which estimates the r_2 is getting lower than r_1. Thus, the interference peaks are gradually vanished when *RI* of surrounding is approaching to that of silica fibers. This is because the Fresnel reflection (r_2) from the interface of fiber/liquid is extremely weak and far different with r_1. In the experimental results of the Fig. 3(b), the peak wavelengths

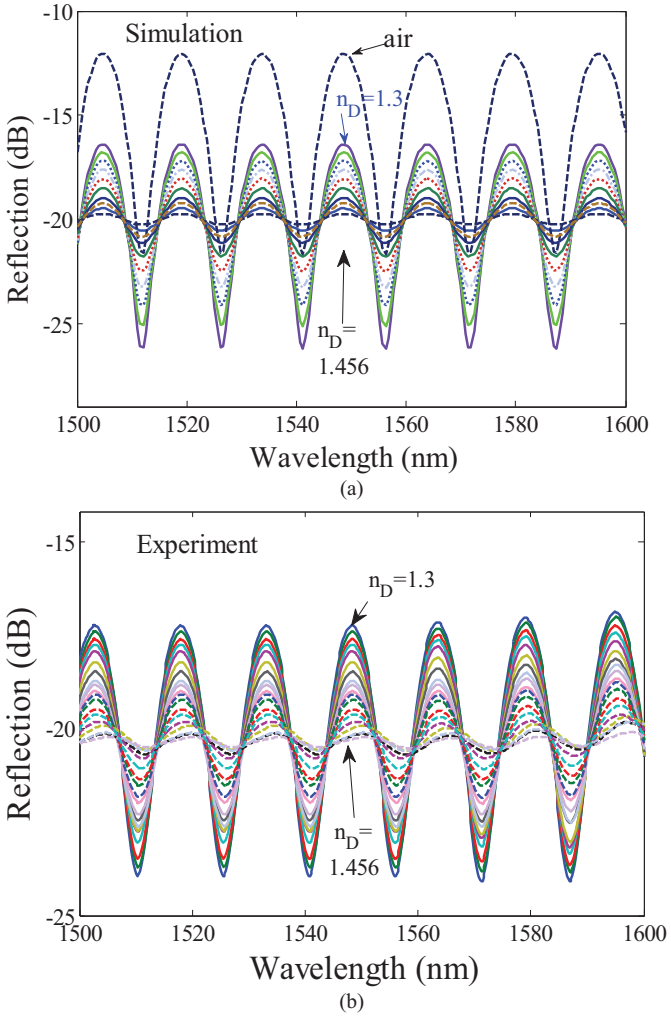

Fig. 3. Interference spectra of (a) simulation and (b) experiment for the proposed device with $d = 55$ μm as RI varies.

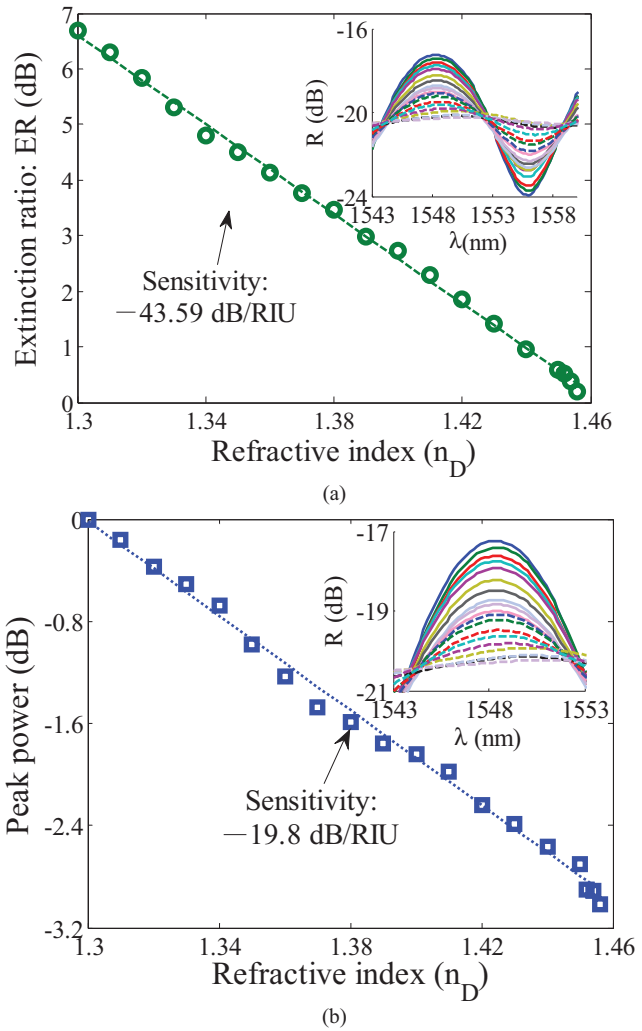

Fig. 4. Experimental sensitivities of the proposed MCFFPI with $d = 55$ μm measured on (a) extinction ratio of interference fringes and (b) reflection power of the peaks. Insets: monitored fringes of the spectra.

of the interference spectra are almost fixed but only the peak attenuation appeared. The experimental results are almost in a good agreement with the calculated results in the Fig. 3(a). It is also observed that the linear changes in the ER and peaks power to the external *RI* that makes the MCFFPI a particularly good refractometer especially in the water based bio/chemical substances for bio/chemical sensing applications.

Fig. 4 (a) plots the RI sensitivity of the 55μm-MCFFPI by monitoring the ER values of the interference fringes. Clearly, a good sensitivity with linear response between the fringe ER and RI is investigated experimentally. The RI sensitivity of −43.59 dB/RIU (around $\lambda = 1550$ nm) is achieved in this case and it can be greatly enhanced if an original MCFFPI with optimized conditions having higher ER of interference fringes. Moreover, the sensing results also can be evaluated by monitoring the peak power of the fringes. Therefore the power can be readily measured by a low cost photo-detector at a certain wavelength. Fig. 4(b) shows the relationship between the peaks power and the external RI of the surrounding. The variations are measured with corresponding to the initial condition at $n_D = 1.3$. Experimental results also indicate a good linearity of response with the peak power sensitivity with −19.8dB/RIU. The measured peaks of spectral fringes are shown in the insets, respectively.

In addition to the properties of miniaturization, all-fiber, simple fabrication, high stability, unnecessary alignment and suitable for external RI measurement, the proposed MCFFPI has a preferable characteristic for high T sensing application. Comparing with those used materials in the MCFFPIs of the previous works [5], [7]–[8], this ultrathin Au embedded MCFFPI can sustain higher T measurement due to the high melting point of the metal Au (>1000 °C).

The high T measurements are performed and the sensitivities of wavelength shifts are shown in the Fig. 5(a). Experimental results show that the interference fringe shifts to long wavelength region while T increases from 25 °C to 800 °C due to the thermal expansion of the F-B cavity. The measured T sensitivity of average +13 pm/ °C displays repeatability and a good linearity performance for many cycles of measurements. The sensor was also placed in the high T of fixed 800 °C for a long term testing. The result shows the interference dips almost fixed for 5 hours which is plotted

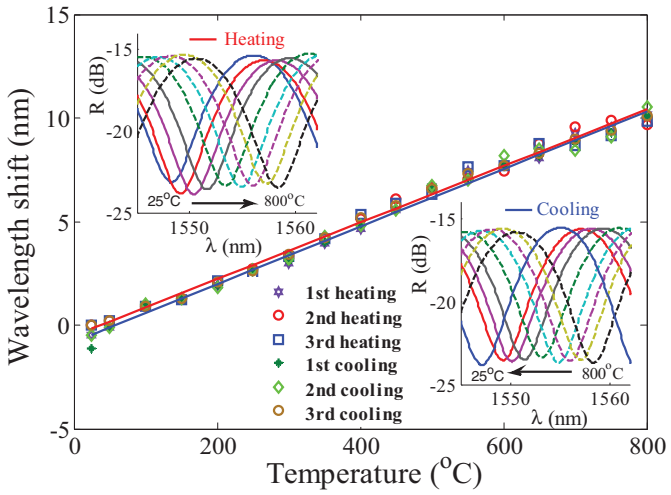

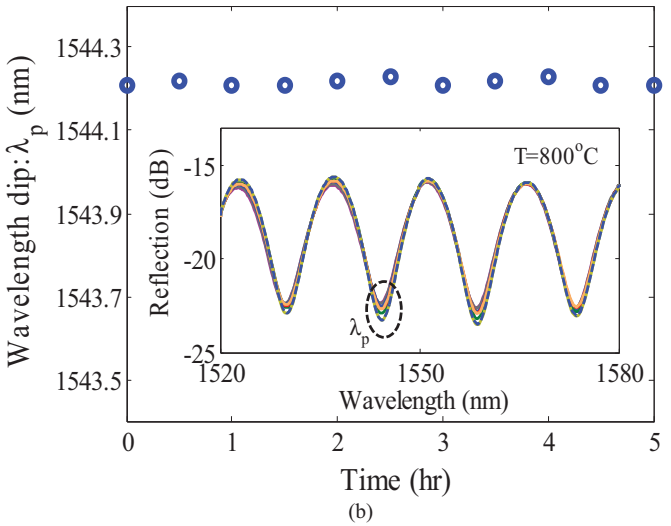

Fig. 5. (a) Wavelength shifts sensitivities of heating and cooling processes for many times of measurements. Insets: wavelength dip variations for the T up and down measurements. (b) Spectral stability of the device in a high T measurement with fixed T = 800 °C. Inset: spectral variation for the long-term sensing.

in the inset of the Fig. 5(b). The results of the Fig. 5(b) demonstrate a stability response in the high T of 800 °C for a long time. From the summary results of the T measurements in the Fig. 5, robust, permanent structure and solid cavity are the main superiorities of the device which causes the optical characteristics and sensing performances still remained the same even after several months and many times of measurements.

IV. Conclusion

We have proposed a miniature Au ultrathin film embedded microcavity fiber Fabry–Pérot interferometer (MCFFPI) and utilized it to measure the external RI and surrounding T. The proposed MCFFPIs with arbitrarily F-B cavity lengths have been fabricated. Measurements reveal that a high sensitivity of −43.59dB/RIU for the extinction ratio measurement is achieved in the external RI sensing. The reported sensor is also suitable for high T measurement with a good linearity response of the sensitivity. The experimental results have investigated the reliability and feasibility of the fiber sensor configuration. It would be further applied to simultaneously measure the external RI and surrounding T. Due to easy fabrication and high chemical stability of the used metal (Au) in the device, we anticipate the proposed sensor will have a variety of applications in chemical and biological sensing fields.

References

[1] O. Frazão, *et al.*, "Fabry–Pérot refractometer based on an end-of-fiber polymer tip," *Opt. Lett.*, vol. 34, no. 16, pp. 2474–2476, Aug. 2009.
[2] Y. J. Rao, M. Deng, D. W. Duan, and T. Zhu, "In-line fiber Fabry–Pérot refractive-index tip sensor based on endlessly photonic crystal fiber," *Sens. Actuators A, Phys.*, vol. 148, no. 1, pp. 33–38, Nov. 2008.
[3] Z. L. Ran, Y. J. Rao, W. J. Liu, X. Liao, and K. S. Chiang, "Laser-micromachined Fabry–Pérot optical fiber tip sensor for high-resolution temperature-independent measurement of refractive index," *Opt. Express*, vol. 16, no. 3, pp. 2252–2263, Feb. 2008.
[4] Z. L. Ran, Y. J. Rao, J. Zhang, Z. Liu, and B. Xu, "A miniature fiber-optic refractive-index sensor based on laser-machined Fabry–Pérot interferometer tip," *J. Lightw. Technol.*, vol. 27, no. 23, pp. 5426–5429, Dec. 1, 2009.
[5] C.-L. Lee, L.-H. Lee, H.-E. Hwang, and J.-M. Hsu, "Highly sensitive air-gap fiber Fabry–Pérot interferometers based on polymer-filled hollow core fibers," *IEEE Photon. Technol. Lett.*, vol. 24, no. 2, pp. 149–151, Jan. 15, 2012.
[6] T. Zhu, T. Ke, Y. J. Rao, and K. S. Chiang, "Fabry–Pérot optical fiber tip sensor for high temperature measurement," *Opt. Commun.*, vol. 283, no. 9, pp. 3683–3685, Oct. 2010.
[7] C.-L. Lee, C.-H. Hung, C.-M. Li, and Y.-W. You, "Simple air-gap fiber Fabry–Pérot interferometers based on a fiber endface with Sn-microsphere overlay," *Opt. Commun.*, vol. 28, no. 26, pp. 4395–4399, Nov. 2012.
[8] C.-L. Lee, W. F. Liu, Z.Y. Weng, and F. C. Hu, "Hybrid AG-FFPI/RLPFG for simultaneously sensing refractive index and temperature," *IEEE Photon. Technol. Lett.*, vol. 23, no. 17, pp. 1231–1233, Sep. 1, 2011.
[9] X. Wang, J. Xu, Y. Zhu, K. Cooper, and A. Wang, "All-fused-silica miniature optical fiber tip pressure sensor," *Opt. Lett.*, vol. 31, no. 7, pp. 885–887, Apr. 2006.
[10] Y. Zhu, K. Cooper, G. Pickrell, and A. Wang, "High-temperature fiber-tip pressure sensor," *J. Lightw. Technol.*, vol. 24, no. 2, pp. 861–869, Feb. 2006.
[11] F. C. Favero, *et al.*, "Spheroidal Fabry–Pérot microcavities in optical fibers for high-sensitivity sensing," *Opt. Express*, vol. 20, no. 7, pp. 7112–7118, Mar. 2012.
[12] L. H. Chena, *et al.*, "Chitosan based fiber-optic Fabry–Pérot humidity sensor," *Sens. Actuators B, Chem.*, vol. 169, no. 5, pp. 167–172, Jul. 2012.
[13] F. Guo, *et al.*, "High-sensitivity, high-frequency extrinsic Fabry–Pérot interferometric fiber-tip sensor based on a thin silver diaphragm," *Opt. Lett.*, vol. 37, no. 9, pp. 1505–1507, May 2012.
[14] C. E. Lee and H. F. Taylor, "Interferometric optical fiber sensors using internal mirrors," *Electron. Lett.*, vol. 24, no. 4, pp. 193–194, Feb. 1988.
[15] M. Naci Inci, S. R. Kidd, and J. S. Barton, "High temperature miniature fiber optic interferometric thermal sensors," *Meas. Sci. Technol.*, vol. 4, no. 3, pp. 382–387, Mar. 1993.